

Characterization and simulation of surface and line-edge roughness in photoresists

V. Constantoudis

Institute of Microelectronics, NCSR "Democritos," 15310, Agia Paraskevi, Greece and Physics Department, National Technical University, Athens, Greece

E. Gogolides,^{a)} G. P. Patsis, and A. Tserepi

Institute of Microelectronics, NCSR "Democritos," 15310, Agia Paraskevi, Greece

E. S. Valamontes

Technological Educational Institute of Athens, Aegaleo, 12210, Greece

(Received 1 June 2001; accepted 1 October 2001)

The problem of surface and line-edge roughness characterization and prediction is discussed. Different roughness parameters, such as the root mean square deviation (rms or σ), the fractal dimension, and the Fourier spectrum, are presented and compared. These roughness parameters for three negative tone resists (wet and plasma developed) are analyzed versus exposure dose, photoacid generator concentration, and plasma development conditions. Finally, a molecular type simulator is used to predict the experimental roughness behavior. © 2001 American Vacuum Society.

[DOI: 10.1116/1.1420582]

I. INTRODUCTION

Since the lithographic processes for this decade are facing the demands of sub-100 nm range characteristic dimension, the roughness of lithographic materials starts playing a significant role in the quality of the printed lines and the critical dimension (CD) control. CD metrology tools can now evaluate line edges and provide a 3σ line edge roughness (LER), which shows the importance of the subject. In the last few years several works¹⁻¹¹ have appeared in the literature studying different aspects of this problem. However, many relevant questions still remain open motivating further work in the field. In this article, we focus our attention on three unanswered questions. First, what are the important roughness parameters, which provide the best and most complete description of a profile or a surface? Second, how do different material properties and process conditions influence these roughness parameters? Third, how can one simulate the roughness formation at the molecular level?

The following discussion consists of three main sections. Each one of them is devoted to one of the above questions. Section II deals with three roughness parameters, namely root mean square deviation σ , fractal dimension D_F , and frequency spectrum. It discusses their advantages and disadvantages as well as their possible interrelations. In Sec. III the behavior of the roughness parameters (σ , D_F) is investigated for experimental surfaces of different materials and process conditions. In Sec. IV we proceed to the implementation of a molecular type simulator following the different steps of the lithography process.

II. ROUGHNESS PARAMETERS

A remaining crucial issue in roughness studies is the lack of a formalism that can describe a real, irregular curve or

surface accurately and uniquely. This is why a lot of methods and parameters for the roughness characterization have been used in the past. However, in the field of lithography the most commonly used parameter is the root mean square deviation σ (usually 3σ values are reported):

$$\sigma = \sqrt{\frac{1}{N} \sum_{i=1}^N (z_i - Z_{av})^2},$$

where z_i are the heights of the line or surface points and N is their total number.

Obviously, the great advantage of σ is that it can be calculated easily. Many scanning electron microscopy and atomic force microscopy (AFM) instruments provide algorithms for calculating σ automatically. On the other hand, σ seems to suffer from two disadvantages. First, it depends on the scale of the measurement and hence different sampling lengths may yield different values for the same profile or surface.⁶ Therefore, one has to distinguish between low frequency and high frequency roughness. This idea has already been used in the metrology method proposed by Winkelmeier *et al.*⁷ The second limitation has to do with the fact that σ only provides information on the important "vertical" magnitude of the roughness without giving any spatial information. It says nothing about the "horizontal" complexity of surfaces or profiles.

A way to obtain more information about the spatial complexity is to introduce fractal geometry.¹² Fractal geometry is an extension of Euclidian geometry, which studies geometrical objects with a self-similar structure by using the notion of noninteger dimension. This dimension, referred to as fractal dimension D_F , is limited by an upper or lower bound; a rough fractal profile will have $1 \leq D_F \leq 2$ depending on how much area it fills, and a two-dimensional fractal surface will have $2 \leq D_F \leq 3$ depending on how much volume it occupies.

^{a)}Electronic mail: evgog@imel.democritos.gr

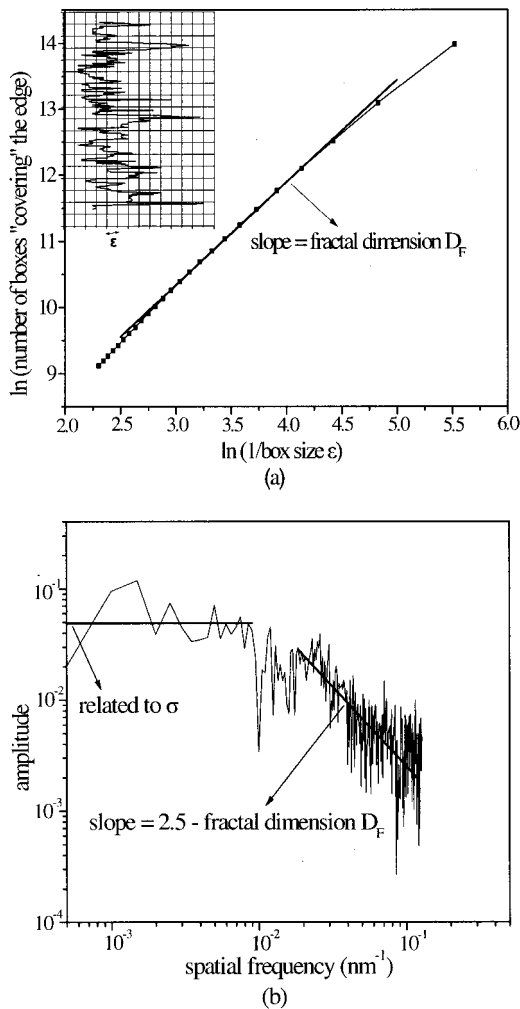


FIG. 1. (a) Estimation of the fractal dimension D_F of the profile shown in the inset. (b) Fourier amplitude spectrum of a typical AFM line scan of a negative tone resist. Notice the different behavior at low and high frequencies as well as the relations with σ and D_F .

In the case of digitized profiles or surfaces, where only a limited set of data points is known, the calculation of D_F needs careful implementation. In the following we will estimate D_F by using the variation method proposed by Dubuc *et al.*,¹³ since they have shown the superior performance of this method compared to other methods when applied to digitized profiles or surfaces. In fact, the variation method provides a new way of counting the total number of boxes (cubes) N required to entirely cover the profile (surface) as a function of the size of the box (cube) ε . The D_F will be the slope of any linear region of the plot of $\ln[N(\varepsilon)]$ versus $\ln(1/\varepsilon)$ [see Fig. 1(a)].

Another traditional method, providing information on the structure of a profile or a surface at different frequency regimes, is the Fourier transform. In Fig. 1(b), the amplitudes of the Fourier transform of a typical AFM line scan of a negative tone photoresist are shown. We observe that it roughly consists of two parts, a horizontal of constant amplitude at low frequencies and a power-law behavior at higher

frequencies. The amplitude of the horizontal part is related to the value of σ .

Moreover, according to the fractal theory,¹² the exponent d of the power law in the spectrum of the amplitudes is related to D_F according to the relation $d = 2.5 - D_F$. However, it has been shown¹⁴ that the accurate estimation of the D_F from the exponent of the power law in the Fourier transform requires a large number of data points (more than 1000), which is not the case for the profiles we get from lithography metrology. For surfaces, a statistical analysis of the Fourier transform of many profiles (sections of the surface) has to be performed which is too time consuming.

Therefore we may infer that although theoretically σ and D_F are linked to different features of the Fourier transform, for experimental surfaces and profiles, inspecting the Fourier spectrum is not a reliable and safe way to estimate them. For this reason, in the following, we will restrict ourselves to the investigation of σ and D_F characterizing the “vertical” and “horizontal” dimension of the roughness correspondingly.

III. ROUGHNESS OF EXPERIMENTAL SURFACES

In this section we will present the results from the calculation of the roughness parameters σ and D_F for various resist surfaces. Our aim is to investigate the effect of different materials and process parameters as well as the possible interrelations between the behavior of two roughness parameters. Most of the measurements were taken with a Digital Instruments Nanoscope III AFM in the noncontact mode. The scan size of the surfaces analyzed was $2 \times 2 \mu\text{m}^2$ and the grid lines 512. Surfaces after high density plasma etching were analyzed with a Topometrix TMX 2000 in the contact mode. The scan size of the surfaces analyzed was $1 \times 1 \mu\text{m}^2$ and the grid lines 300. Comparison between instruments showed little difference in the measurements.

Let us start with the surface roughness (SR) of a wet developed negative tone epoxy resist (EPR). This resist is extremely sensitive to electron-beam and to deep ultraviolet radiation and is developed with organic solvents.¹⁵ A modified version of EPR can be developed with standard aqueous developer and is promising for micromachining applications.¹⁶ EPR with a 1% photoacid generator (PAG) concentration was used prebaked at 110°C , electron-beam exposed at 50 keV to form $10 \times 10 \mu\text{m}^2$ pads, postexposure baked at 100°C , developed in propylene glycol methyl ether acetate (PGMEA), and measured in the AFM. Analysis of the measurements was done with the methods described in Sec. II. Figure 2 shows the dependence of σ and D_F on exposure dose in the region $1.0\text{--}4.0 \mu\text{C}/\text{cm}^2$ (experimental values). Two observations could be made. First, we observe that the σ goes through a maximum at low doses, i.e., at the onset of the contrast curve. As the dose increases, the σ drops quickly up to $2 \mu\text{C}/\text{cm}^2$ and then continues decreasing but with a lower rate. On the contrary, the behavior of D_F seems to be the opposite. It increases following the increase in exposure dose. Here we can also distinguish two regions: at doses lower than $2 \mu\text{C}/\text{cm}^2$, D_F increases quickly, whereas at higher doses the increase is slower.

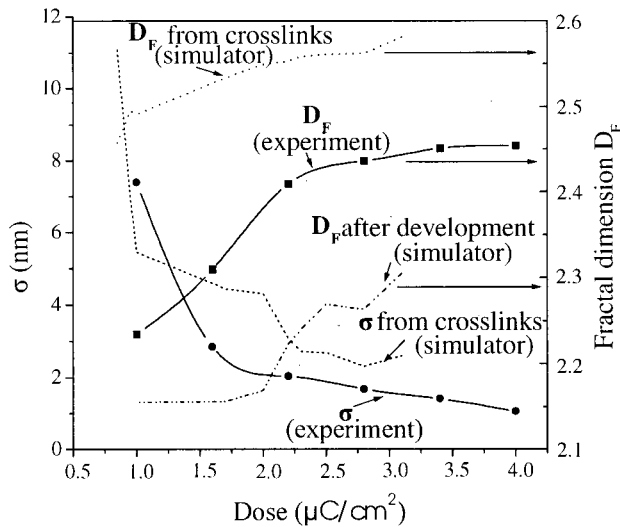


FIG. 2. Experimental values of σ and D_F vs exposure dose for negative tone epoxy resist with 1% PAG. In addition, the corresponding σ (from crosslinks positions) and D_F (before and after development) predicted by simulation are shown. The σ by simulation after development over predicts the experimental value and is not shown. Note the opposite behavior of σ and D_F vs exposure dose and the qualitative agreement between experiment and simulation.

The same behavior has been observed in the second type of surfaces we analyzed. These come from a negative tone siloxane resist with oxygen plasma development in a high-density plasma (HDP) reactor (Alcatel MET inductively coupled plasma reactor). In particular, the resist is a commercial polydimethyl siloxane (PDMS) by Aldrich with a broad MW distribution ($M_n = 60\,000$, $M_w/M_n = 2$).⁸ The resist was coated on hard baked novolac at approximately 100 nm thickness. Although the resist without any sensitizer is very sensitive to 157 nm radiation, here it was exposed with 50 keV electrons and developed in methyl isobutyl ketone (MIBK). After wet development of the siloxane top layer, oxygen plasma development of the bottom layer followed in the HDP reactor (conditions: 10 mTorr, 100 sccm oxygen flow, source power 600 W, bias 100 V). A break-through step (BTS) containing fluorinated gases and oxygen preceded the pure oxygen plasma development. In this case we will examine not only the effect of exposure dose on SR, but also the effect of the bias voltage during the BTS. Figure 3 shows the results of these dependencies for σ and D_F . Both σ curves exhibit similar behavior with the difference that at useful doses the σ in the no-bias voltage case takes slightly lower values than the σ in the case of 100 V bias voltage. This is an indication that the BTS should be conducted without bias for better SR and LER behavior. The D_F of both surfaces, at low doses, increases quickly and then displays a broad maximum before starting slightly to decrease at high doses. Generally, we observe for a second time that σ and D_F behave in an opposite way; when the first decreases the second increases.

In an effort to examine the influence of the reactor type on the roughness of plasma developed siloxane resists, we repeated the experiments in a reactive ion etching (RIE) reac-

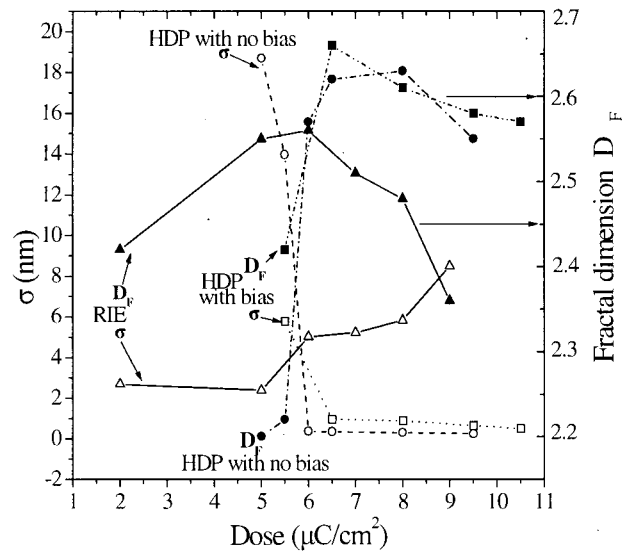


FIG. 3. Dependence of σ and D_F of a negative tone plasma developed resist on exposure dose, type of reactor, and bias voltage during the breakthrough step. Notice: (i) the difference between HDP and RIE results, (ii) the behavior of σ with and without bias voltage (BTS step in HDP), and (iii) the trend towards opposite behavior of σ and D_F .

tor, and show the remarkably different results in Fig. 3. Whereas at low doses ($\leq 5 \mu\text{C}/\text{cm}^2$), σ decreases and D_F increases versus dose, at higher doses σ starts rising and D_F decreasing (for dose $> 6.5 \mu\text{C}/\text{cm}^2$) in contrast with the behavior observed in the HDP. The molecular details and the possible explanations of this behavior will be discussed elsewhere, although we can hypothesize that the good temperature control in the HDP reactor is the reason for this difference and better performance of the HDP reactor. Here we only point out the important role the type of reactor plays in the roughness behavior of resist surfaces. Moreover, by inspecting the RIE curves in Fig. 4, we also infer the opposite behavior that σ and D_F exhibit versus exposure dose.

IV. MOLECULAR SIMULATION OF ROUGHNESS FORMATION AND COMPARISON WITH EXPERIMENTAL RESULTS

Besides the roughness studies of experimental surfaces, it is worthwhile attempting a molecular type simulation following the different steps of the lithographic process. Obviously, such a simulation tool will be useful in providing a first order prediction of the optimum choices of material properties and process conditions. The simulator was first developed for the epoxy resist EPR discussed in the previous section. Its principles and its first application for roughness studies have already been presented^{9,10} before. In the following, using our simulator,⁹ we examine the dependence of the roughness parameters, σ and D_F , on the exposure dose, PAG concentration, and development process.

As regards the dependence on exposure dose, we restrict ourselves to the case where PAG concentration equals 5%.

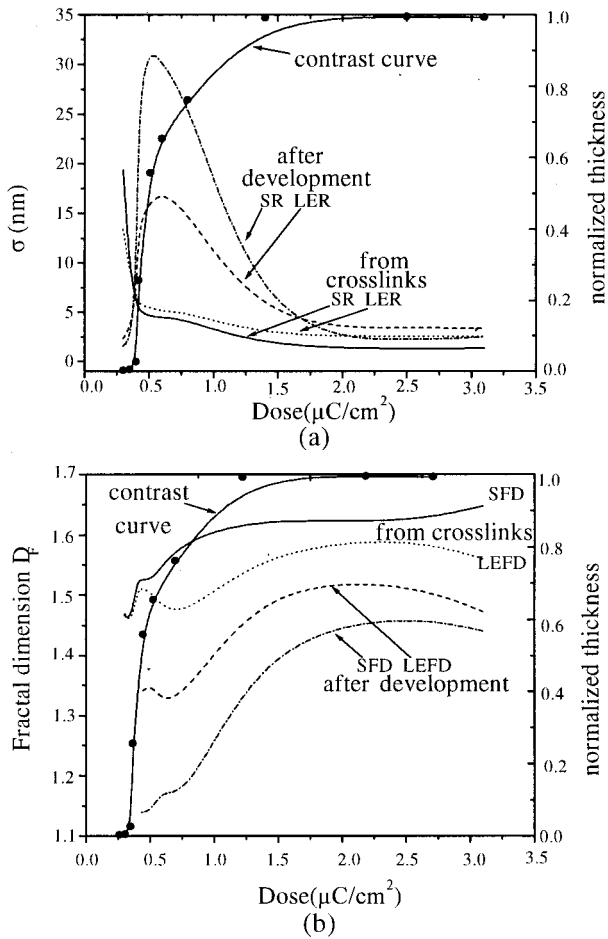


FIG. 4. Dependence of σ roughness (a) and fractal dimension D_F (b) for surface (SR and SFD) and line profiles (LER and LEFD) before and after development on exposure dose. The PAG content was set equal to 5%.

Similar results are obtained for other PAG contents. In Fig. 4, we show roughness (σ) and fractal dimension (D_F) for surfaces and line edges [SR and LER in Fig. 4(a), as well as SFD and LEFD in Fig. 4(b), respectively] before and after development as a function of exposure dose, as well as the contrast curve. Our result show that σ (SR and LER) goes through a peaked maximum at very low doses and then quickly drops to small values at useful doses. In fact, the maximum roughness from cross-link positions is situated at the onset of the contrast curve. On the contrary, at low doses D_F follows the rise in the contrast curve and then is almost stabilized at useful doses. Furthermore, the development process seems to increase σ of both SR and LER, whereas the opposite holds for D_F . We note here that our development model is applied for organic development of EPR.⁹

Figure 5 shows the effects of PAG content on roughness (σ) and fractal dimension (D_F) for surface and line edge profiles [SR and LER in Fig. 5(a), as well as SFD and LEFD in Fig. 5(b), respectively] produced from our simulator. Results are shown before and after development at high doses different for each PAG content. One can observe that increasing the PAG content is followed by a decrease in σ and an

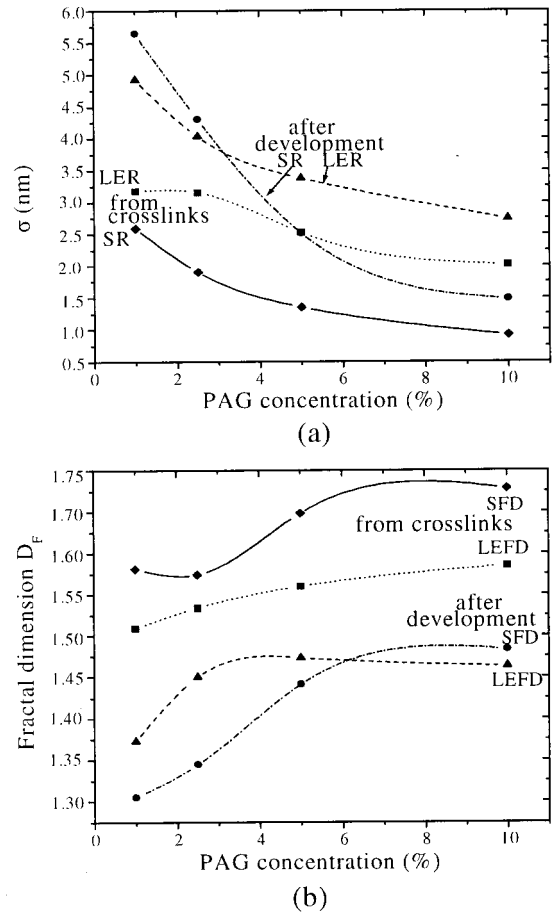


FIG. 5. σ (a) and D_F (b) for surface (SR and SFD) and line profiles (LER and LEFD) vs PAG concentration for high exposure doses. Notice again the opposite behavior of σ and D_F : as the PAG content increases, the former is reduced whereas the latter is slightly increased.

increase in D_F . For this cross-linking system, high PAG content induces high cross-linking and reduces acid diffusion length. This has two effects: On the one hand, profiles cannot show large rough fluctuations, thus σ is reduced. On the other hand, the acid catalyzed reactions take place in smaller areas, increasing the local cross-link density and thus triggering the appearance of more important small-scale structure in profiles, which are made more complex. The increase in complexity is quantified by the increase in fractal dimension observed in Fig. 5(b).

Let us proceed in the comparison of the simulator results for σ and D_F with the experimental ones. Figure 2, apart from the experimentally measured σ and D_F values for EPR surfaces with 1% PAG content, shows the corresponding simulator results. The σ value of the cross-link positions predicted by our simulator follows closely the experimental value. On the contrary, the σ value after development (not shown here) overpredicts the experimental value, which is a hint that our simplified development model is too aggressive for mildly cross-linked systems.⁹

As regards the fractal dimension, we can observe that all D_F curves in Fig. 2 exhibit a monotonic increasing behavior

as dose increases. Therefore qualitatively there is an agreement between experimental and simulator results for the D_F and σ values confirming that the simulator has captured the main mechanisms of the lithography process in negative tone resists.

V. SUMMARY AND CONCLUSIONS

In this article, the problem of roughness in photoresists was addressed by inspecting three relevant aspects: (i) quantitative characterization, (ii) dependence on some material properties and process conditions, and (iii) molecular simulations.

(i) In the context of roughness characterization, three different parameters (σ , fractal dimension D_F , and Fourier spectrum) were described and compared to each other. In particular, we clarified that theoretically some features of the form of the Fourier transform of a profile can be related with σ and D_F values. However, in practice for digitized profiles the accurate estimation of D_F from Fourier transform requires a lot of data points to be known, which is not the case in lithography metrology. Therefore the only useful information we can get from the Fourier transform has been the region of scales where self-similarity occurs and hence fractal analysis can be applied.

(ii) As regards the dependence of roughness on material properties and process conditions, we studied three different negative tone resists with both wet and dry development. We concluded that:

(1) The behavior of σ and D_F seems to be interrelated. Although theoretically σ and D_F can characterize a profile or a surface independently to each other,¹¹ for the experimental surfaces we studied this is not totally true. σ and D_F exhibit opposite behavior, especially when they are studied versus exposure dose. This means that generally when one of them increases (decreases) the other decreases (increases). By close inspection of experimental curves we can find some exceptions, but the general trend is the above mentioned.

(2) The type of plasma reactor (RIE or HDP) plays a crucial role in the quality of the printed line. At useful doses, the use of HDP with good temperature control of the wafer led to lower σ values than the use of RIE. This very interesting phenomenon is under investigation and details will be presented elsewhere.

(iii) A molecular type simulator of the different steps of the lithography process was constructed for a negative tone resist, and the behavior of σ and D_F versus exposure dose and PAG content was studied. We concluded that our molecular simulator reproduces the opposite behavior of σ and D_F , which was observed in experimental surfaces. This behavior can be understood by the following argument: At very small doses (not accessible by experimental measurements), the polymer is not cross-linked and thus roughness and surface complexity are small leading to small σ and D_F . At high doses, the polymer is cross-linked and not attacked by the developer (σ small). However, cross-linking gives surface complexity and so a high D_F . At intermediate doses, low cross-linking results in attack of the surface by the developer and thus leads to large σ and intermediate D_F .

ACKNOWLEDGMENTS

The financial support of the ESPRIT Project No. 33562 "RESIST 193-157" and the Greek Project No. PENED 99ED56 is kindly acknowledged. The authors thank Dr. I. Raptis for his help with electron-beam exposures.

¹H. Namatsu, M. Nagase, T. Yamagushi, K. Yamazaki, and K. Kuriharo, *J. Vac. Sci. Technol. B* **16**, 3315 (1998).

²D. He and F. Cerrina, *J. Vac. Sci. Technol. B* **16**, 3748 (1998).

³W. G. Reynolds and W. J. Taylor, *J. Vac. Sci. Technol. B* **17**, 2723 (1999).

⁴T. Azumo, K. Chiba, M. Imabeppu, D. Kawamura, and Y. Onishi, *Proc. SPIE* **3999**, 264 (2000).

⁵S. Masuda, X. Ma, G. Noya, and P. Pawlowski, *Proc. SPIE* **3999**, 252 (2000).

⁶L. Spanos and E. A. Irene, *J. Vac. Sci. Technol. A* **12**, 2646 (1994).

⁷S. Winkelmeier, M. Sarstedt, M. Ercken, M. Goethals, and K. Ronse, *Microelectron. Eng.* **57-58**, 665 (2001).

⁸A. Tserepi, E. S. Valamontes, E. Tegou, I. Raptis, and E. Gogolides, *Microelectron. Eng.* **57-58**, 547 (2001).

⁹G. P. Patsis and E. Gogolides, *Microelectron. Eng.* **57-58**, 563 (2001).

¹⁰G. P. Patsis, A. Tserepi, I. Raptis, N. Glezos, E. Gogolides, and E. S. Valamontes, *J. Vac. Sci. Technol. B* **18**, 3292 (2000).

¹¹L. Lai and E. A. Irene, *J. Vac. Sci. Technol. B* **17**, 33 (1999).

¹²M. H. Hastings and G. Sugihara, *Fractals* (Oxford Science, Oxford, 1994).

¹³B. Dubuc, J. F. Quiniou, C. Rocques-Carmes, C. Tricot, and S. W. Zucker, *Phys. Rev. A* **39**, 1500 (1989).

¹⁴M. W. Mitchell and D. A. Bonnell, *J. Mater. Res.* **5**, 2244 (1990).

¹⁵P. Argitis, I. Raptis, C. J. Aidinis, N. Glezos, M. Bacciochi, J. Everett, and M. Hatzakis, *J. Vac. Sci. Technol. B* **13**, 3030 (1995).

¹⁶I. Raptis, M. Chatzichristidi, C. D. Diakoumakos, A. Douvas, D. Niakoula, and P. Argitis, *J. Photopolym. Sci. Technol.* **14**, 445 (2001).